NASA
Technical
Paper
3178

December 1991

A Nonlinear Estimator for Reconstructing the Angular Velocity of a Spacecraft Without Rate Gyros

M. E. Polites
and W. D. Lightsey

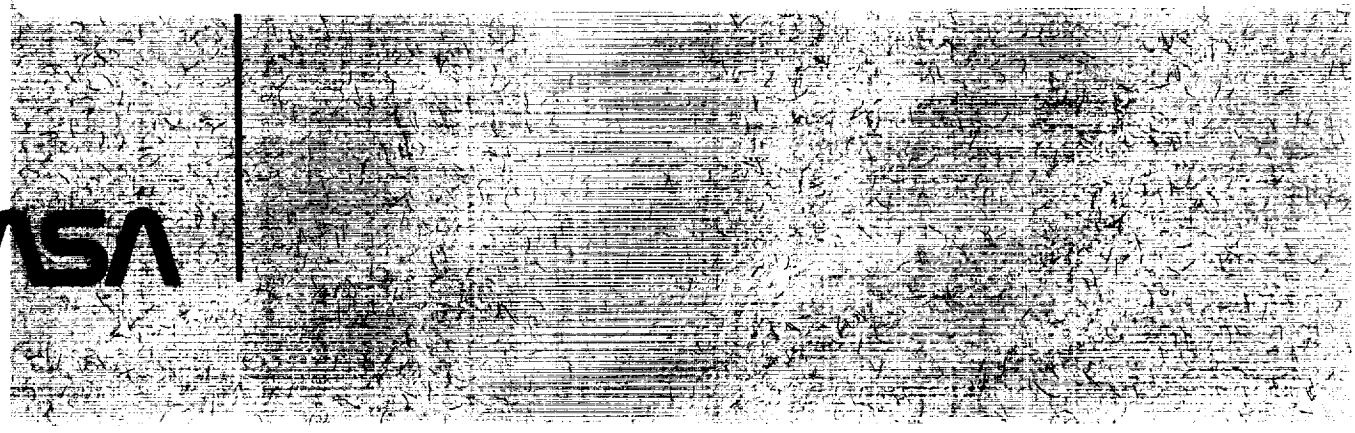

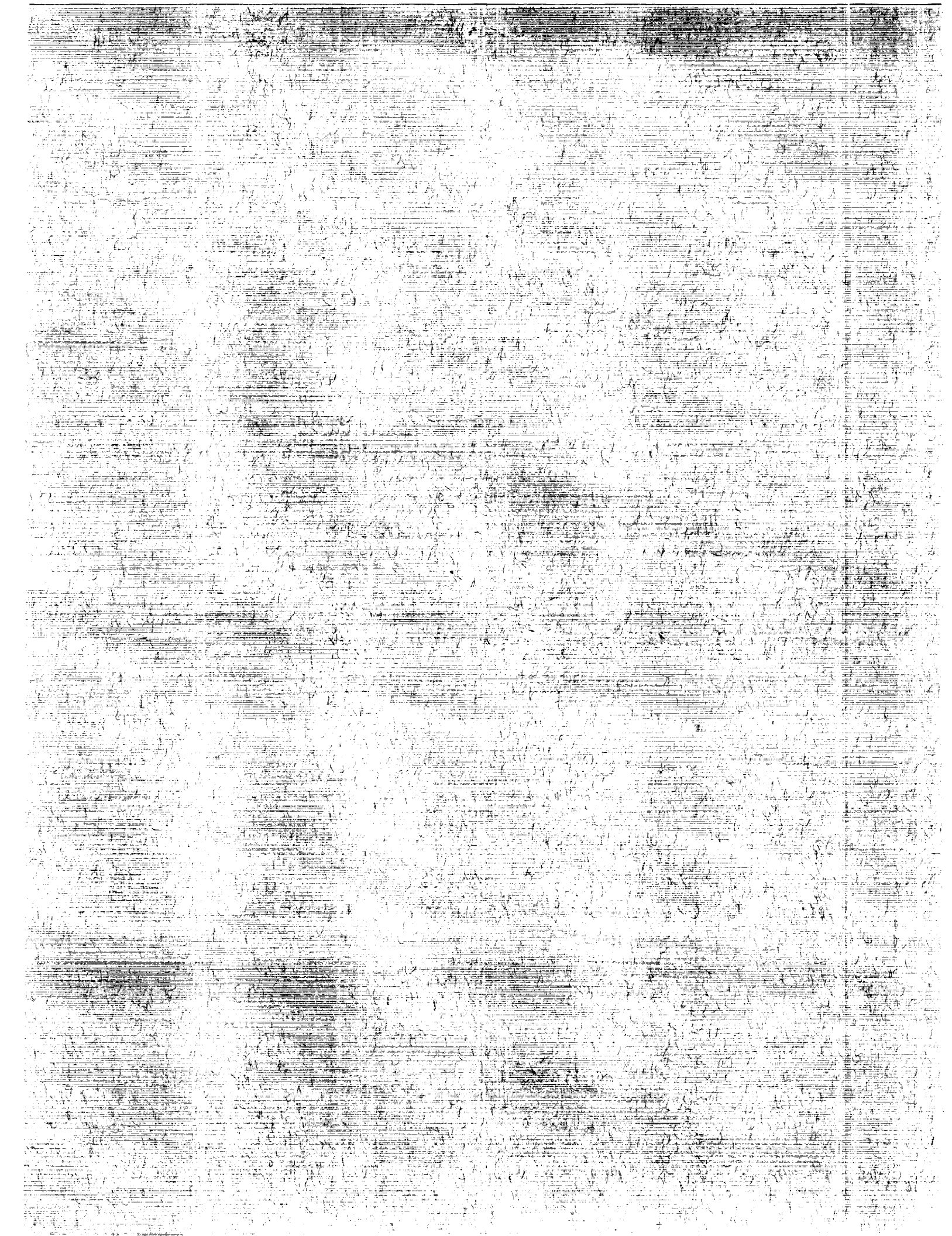

NASA Technical Paper 3178

1991

A Nonlinear Estimator for Reconstructing the Angular Velocity of a Spacecraft Without Rate Gyros

M. E. Polites
and W. D. Lightsey
George C. Marshall Space Flight Center
Marshall Space Flight Center, Alabama

National Aeronautics and Space Administration
Office of Management
Scientific and Technical Information Program

TABLE OF CONTENTS

LIST OF ILLUSTRATIONS

TECHNICAL PAPER

A NONLINEAR ESTIMATOR FOR RECONSTRUCTING THE ANGULAR VELOCITY OF A SPACECRAFT WITHOUT RATE GYROS

I. INTRODUCTION

In a spacecraft attitude control system, vehicle angular velocity is normally needed for rate damping to stabilize the system. Sometimes it is integrated to give vehicle attitude, which is updated periodically by onboard sensors like Sun sensors or star trackers. In determining angular velocity, the standard procedure is to measure it using a set of three or more body-mounted rate gyros. However, rate gyros have shown a tendency to fail in the past. Take, for example, the rate gyro failures on such spacecraft as Skylab,[1] the International Ultraviolet Explorer,[2] and more recently the Hubble space telescope (HST).[3] When this happens, there is invariably a need to estimate angular velocity using other onboard sensors in order to maintain vehicle control. Differentiating the outputs from a Sun sensor or a star tracker is a standard approach, but this does not work for all spacecraft attitudes, since it requires that the Sun or a reference star, respectively, be in the linear range of the sensor at all times. Also, this gives only angular velocity in the plane normal to the sensor boresight. Reconstructing it along with vehicle attitude using a Kalman filter, and perhaps a Sun sensor/star tracker or else two star trackers, is another approach. However, this requires linearization of the vehicle equations of motion, one way or another, and usually requires some initial knowledge of vehicle attitude for reference star identification.[2,4–8]

This paper presents a new scheme for estimating spacecraft angular velocity that has none of these problems. It works for all spacecraft attitudes, does not require any linearization of the vehicle equations of motion, and requires no knowledge of vehicle attitude. It is based upon a nonlinear estimator whose inputs are measured inertial vectors and their calculated time-derivatives relative to vehicle axes. This scheme works well with a variety of onboard sensors, like Sun sensors, star trackers, or magnetometers, and in concert. It can also use look-angle information from onboard tracking antennas for tracking data and relay satellites or global positioning system satellites. It works when vehicle attitude is controlled using a reaction control system (RCS) as well as momentum exchange devices, like control moment gyros (CMG's) or reaction wheels.

The approach to presenting this new estimation scheme is as follows. In section II, it is derived. In section III, it is applied to a Sun point scheme on the HST, assuming four or more of its rate gyros have failed. Simulation results are presented that verify both the estimator and the Sun point scheme which uses it. Final comments are made in section IV.

II. DERIVATION OF THE ANGULAR VELOCITY ESTIMATOR

The angular velocity estimator is structured similar to a Kalman filter. The estimated angular velocity is propagated frequently based on a model of the plant. Periodically, this is updated using measurements from onboard sensors like Sun sensors, star trackers, or magnetometers, to name a few. The algorithms for propagating the estimated angular velocity

based on the plant model will be derived first, followed by the algorithms for the measurement update scheme. The complete scheme is then described, and aspects of its implementation are considered.

A. Estimate Propagated From Plant Model

The equations of motion for the spacecraft are given by[9]

$$\dot{\vec{H}}_V = \vec{T}_C + \vec{T}_D \ , \tag{1}$$

where $\vec{H}_V$ is the angular momentum vector of the vehicle with respect to its center of mass, $\vec{T}_C$ is the control torque vector acting about the center of mass, and $\vec{T}_D$ is the disturbance torque vector acting about the center of mass. It is well known that the components of $\vec{H}_V$ in vehicle axes are related to the components of the spacecraft angular velocity vector $\vec{\omega}_V$ expressed in vehicle axes by the matrix transformation

$$\underline{H}_V = I_V \underline{\omega}_V \ . \tag{2}$$

Here, $\underline{H}_V \in R^3$ contains the components of vehicle angular momentum in vehicle axes, $\underline{\omega}_V \in R^3$ contains the components of spacecraft angular velocity in vehicle axes, and $I_V \in R^{3\times3}$ is the spacecraft inertia matrix, which can be written as

$$I_V = \begin{bmatrix} I_{V11} & I_{V12} & I_{V13} \\ I_{V21} & I_{V22} & I_{V23} \\ I_{V31} & I_{V32} & I_{V33} \end{bmatrix} , \tag{3}$$

relative to vehicle axes. Integrating equation (1) over the interval from t_{n-1} to t_n, expressing the result in matrix form, substituting equation (2) into this, and rearranging, produces

$$\underline{\omega}_V(t_n) = \underline{\omega}_V(t_{n-1}) + I_V^{-1} \left\{ \int_{t_{n-1}}^{t_n} [\underline{T}_C(\xi) + \underline{T}_D(\xi)] \, d\xi \right\} \ . \tag{4}$$

Here, $\underline{T}_C(t)$ and $\underline{T}_D(t)$ contain the components of $\vec{T}_C(t)$ and $\vec{T}_D(t)$ in vehicle axes, respectively. $\underline{T}_D(t)$ is the net torque due to disturbances like aerodynamics, the gravity gradient, and magnetics. Assuming these are low amplitude and low frequency disturbances compared to the control torque $\underline{T}_C(t)$, then over a small enough interval $(t_n - t_{n-1})$, equation (4) can be approximated by

$$\underline{\omega}_V(t_n) \doteq \underline{\omega}_V(t_{n-1}) + I_V^{-1} \int_{t_{n-1}}^{t_n} \underline{T}_C(\xi) d\xi \ . \tag{5}$$

This is the basic algorithm for propagating the estimated angular velocity with an RCS system for control. Knowing the thruster lever arms to the vehicle center of mass, thrust levels, and thruster firings versus time, the integral in equation (5) can be determined. With a set of momentum exchange devices like CMG's or reaction wheels,

$$\vec{T}_C = -\dot{\vec{H}}_{\mathrm{MED}} \ , \tag{6}$$

where $\vec{H}_{\mathrm{MED}}$ is the angular momentum in the momentum exchange devices. Integrating equation (6) from t_{n-1} to t_n and expressing the result in matrix form gives

$$\int_{t_{n-1}}^{t_n} \underline{T}_C(\xi)d\xi = -[\underline{H}_{\mathrm{MED}}(t_n) - \underline{H}_{\mathrm{MED}}(t_{n-1})] \ ,$$

where $\underline{H}_{\mathrm{MED}}(t_n)$ contains the components of $\vec{H}_{\mathrm{MED}}(t_n)$ in vehicle axes. Substituting this into equation (5) produces

$$\underline{\omega}_V(t_n) \doteq \underline{\omega}_V(t_{n-1}) - I_V^{-1}[\underline{H}_{\mathrm{MED}}(t_n) - \underline{H}_{\mathrm{MED}}(t_{n-1})] \ , \tag{7}$$

which is a better form for the propagation algorithm when momentum exchange devices are used for control. With CMG's, $\underline{H}_{\mathrm{MED}}(t_n)$ is determined knowing the momentum vector of each CMG and its direction relative to the vehicle, from gimbal angle measurements. With reaction wheels, it is determined knowing the inertia of each wheel and measuring wheel speeds. In many situations, the spacecraft vehicle axes are nearly aligned with its principal axes, and so, the products of inertia in equation (3) are small compared to the moments of inertia and can be neglected. When this is the case, then I_V^{-1} in equation (5) or (7) can be approximated by

$$I_V^{-1} = \begin{bmatrix} I_{V11}^{-1} & 0 & 0 \\ 0 & I_{V22}^{-1} & 0 \\ 0 & 0 & I_{V33}^{-1} \end{bmatrix} .$$

This uncouples the system of equations in (5) or (7) and simplifies their computation.

B. Estimate Update Scheme

Unfortunately, the estimated spacecraft angular velocity in equation (5) or (7) will deteriorate with time because the external disturbance torque $\underline{T}_D(t)$ is not included; it is assumed to be unknown. Consequently, the estimated angular velocity needs to be updated periodically using measurements from onboard sensors. In this process, the scheme presented here includes the latest estimate for spacecraft angular velocity. This is analogous to the Kalman filter update equation that uses measurements and the latest estimate for the state vector to arrive at an estimate update.

The basic concept of the update scheme is illustrated in figure 1. It shows the noncolinear vectors $\vec{\rho}_1$ and $\vec{\rho}_2$, which are assumed fixed in magnitude and direction relative to the inertial frame (I_1,I_2,I_3). Assume there are sensors onboard the spacecraft whose measurements allow the components of $\vec{\rho}_1$ and $\vec{\rho}_2$, in vehicle axes (V_1,V_2,V_3), to be determined. Also, assume that from a number of these measurements, the time derivatives of these vectors, as seen by an observer rotating with the vehicle frame, can be approximated. These are denoted by $(\dot{\vec{\rho}}_1)_{\mathrm{REL}\,V}$

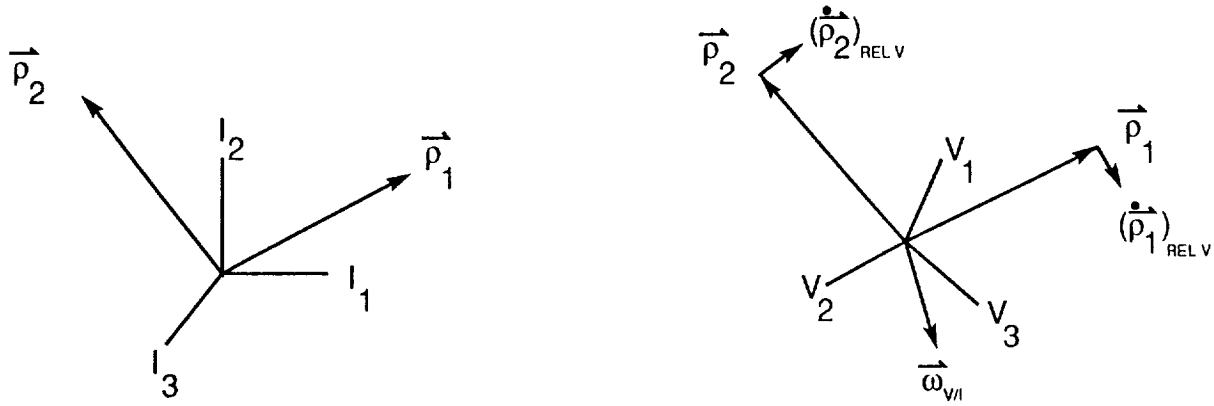

Figure 1. Coordinate systems and inertial vectors that illustrate the basic concept of the update scheme.

and $(\dot{\vec{\rho}}_2)_{REL\ V}$ in the figure. Then intuition says this ought to be enough information to deduce the angular velocity of the vehicle frame relative to the inertial frame, denoted by the vector $\vec{\omega}_{V/I}$ or just $\vec{\omega}_V$ for brevity. This is the case, as will be shown. Furthermore, the concept is not just limited to two inertial vectors, but can be readily extended to N inertial vectors where $N \geq 2$ and at least two are noncolinear. Nor do these measured vectors have to be truly inertial. As long as they change very little in magnitude and direction relative to the (I_1,I_2,I_3) frame over the time between updates, they may have utility. This depends upon how accurately vehicle angular velocity needs to be calculated. Finally, the scheme can and will be augmented with inertial vectors chosen to be aligned with the vehicle axes at the time of an update. Using the latest estimate for the spacecraft angular velocity based on the plant model, their time derivatives relative to the vehicle axes are calculated. This serves several purposes. First, it allows the latest estimate of vehicle angular velocity to be weighted with the effective measured value imbedded in the sensor measurements, a la a Kalman filter. Secondly, it allows one measured inertial vector and its calculated time derivative to partially update the previous estimate for angular velocity without mathematical singularity. The same is true if all measured inertial vectors happen to be colinear. Thirdly, it maintains the mathematical integrity of the scheme when no measurements are available. In this case, the estimates just before and after the update are equal.

The procedure to derive the update algorithms is as follows. It begins with the simple case of a spacecraft that measures the Earth's magnetic field flux density vector and a unit Sun vector in vehicle axes, using an onboard magnetometer and Sun sensors, respectively. The scheme is then augmented with the inertial vectors aligned with the vehicle axes at the time of an update. Extending it to include star trackers or other measurements is straightforward.

A spacecraft in Earth orbit is assumed to have a magnetometer that can measure the components of the flux density vector $\vec{B}$ for the Earth's magnetic field in vehicle axes (B_{V1},B_{V2},B_{V3}). It also has one or more Sun sensors. From their outputs, the direction cosines of a unit Sun vector $\vec{S}$ in vehicle axes (S_{V1},S_{V2},S_{V3}) can be determined. Over the time interval between updates (e.g., 10 s), $\vec{B}$ and $\vec{S}$ are assumed essentially fixed in magnitude and direction relative to an Earth-centered inertial coordinate frame (I_1,I_2,I_3). Then, it follows from basic kinematics that[9]

$$(\dot{\vec{B}})_{\text{REL } V} = \vec{\omega}_{I/V} \times \vec{B} = \vec{B} \times \vec{\omega}_{V/I} = \vec{B} \times \vec{\omega}_V \tag{8}$$

$$(\dot{\vec{S}})_{\text{REL } V} = \vec{\omega}_{I/V} \times \vec{S} = \vec{S} \times \vec{\omega}_{V/I} = \vec{S} \times \vec{\omega}_V \ .$$

First, equation (8) will be normalized by $|\vec{B}|$ to initially give $\vec{B}$ and $\vec{S}$ equal weight, since $\vec{S}$ is a unit vector. Then, both equations are multiplied by the weighting factors k_B and k_S, respectively, to yield

$$\begin{aligned} \frac{k_B(\dot{\vec{B}})_{\text{REL } V}}{|\vec{B}|} &= \frac{k_B \vec{B}}{|\vec{B}|} \times \vec{\omega}_V \\ k_S(\dot{\vec{S}})_{\text{REL } V} &= k_S \vec{S} \times \vec{\omega}_V \ . \end{aligned} \tag{9}$$

This allows relative weights to be appropriately chosen for the situation. For example, during orbit day $k_B = k_S = 1$, whereas during orbit night $k_B = 1$ and $k_S = 0$. The possibility also exists of choosing them to optimize the estimated angular velocity, similar to a Kalman filter. Equation (9) can be written in matrix form as

$$\begin{aligned} \frac{k_B(\dot{\underline{B}})_{\text{REL } V}}{|\underline{B}|} &= \frac{k_B \tilde{\underline{B}}}{|\underline{B}|} \underline{\omega}_V \\ k_S(\dot{\underline{S}})_{\text{REL } V} &= k_S \tilde{\underline{S}}\, \underline{\omega}_V \ , \end{aligned} \tag{10}$$

where the vectors are expressed in terms of their components in vehicle axes and for

$$\underline{A} = \begin{bmatrix} A_1 \\ A_2 \\ A_3 \end{bmatrix},$$

$\tilde{\underline{A}}$ is defined to be

$$\tilde{\underline{A}} = \begin{bmatrix} 0 & -A_3 & A_2 \\ A_3 & 0 & -A_1 \\ -A_2 & A_1 & 0 \end{bmatrix}.$$

Next define

$$\underline{\delta} = \begin{bmatrix} \dfrac{k_B(\dot{\underline{B}})_{\text{REL } V}}{|\underline{B}|} \\ \\ k_S(\dot{\underline{S}})_{\text{REL } V} \end{bmatrix}, \tag{11}$$

and

$$\tau = \begin{bmatrix} k_B \dfrac{\tilde{B}}{|B|} \\ \\ k_S \tilde{S} \end{bmatrix} . \tag{12}$$

From equations (10), (11), and (12),

$$\underline{\delta} = \tau \underline{\omega}_V . \tag{13}$$

Let the estimated angular velocity $\hat{\underline{\omega}}_V$ be given by

$$\hat{\underline{\omega}}_V = [\tau^T \tau]^{-1} \tau^T \underline{\delta} , \tag{14}$$

which is the pseudo inverse of τ times $\underline{\delta}$. Observe from equations (13) and (14) that $\hat{\underline{\omega}}_V = \underline{\omega}_V$, assuming DET$[\tau^T \tau] \neq 0$.

The next step is to determine $\underline{B}$, $(\dot{\underline{B}})_{\text{REL } v}$, $\underline{S}$, and $(\dot{\underline{S}})_{\text{REL } v}$ at the time of each update. A scheme developed by Polites[10] will be utilized here. A logic flow chart for it is shown in figure 2. It takes noisy measurements $\tilde{y}$ of a variable y every ΔT seconds, and inputs them into a two-dimensional recursion formula. After N iterations or $T = N\Delta T$ seconds, the output of the recursion formula $\underline{w} \in R^2$ is multiplied by a constant matrix $Q \in R^{2\times 2}$ that is a function of N and ΔT, to yield the estimates $\hat{y}$ and $\hat{\dot{y}}$ at the end of the T-second interval. In actuality, this is a least-squared error fit of the measurements to a straight line with the computations performed recursively. The following example illustrates how it is applied here. Suppose magnetometer measurements in vehicle axes are generated every $\Delta T = 1$ s, as they are on the Hubble space telescope. Suppose an update to the estimated angular velocity is to occur every $T = 10$ s. Then $N = 10$ consecutive measurements in each axis are input into the recursion formulas, independently, to generate $\underline{B}$ and $(\dot{\underline{B}})_{\text{REL } v}$, every $T = N\Delta T = 10$ s. A similar procedure is used for the components of the unit Sun vector in vehicle axes derived from Sun sensor measurements. However, it is not necessary for the Sun sensor measurements to be generated every $\Delta T = 1$ s too, so long as $\underline{S}$ and $(\dot{\underline{S}})_{\text{REL } v}$ are generated every $T = 10$ s and at the same time as $\underline{B}$ and $(\dot{\underline{B}})_{\text{REL } v}$,. This is a distinct advantage of this approach.

Equation (14) assumes that DET$[\tau^T \tau] \neq 0$, where τ is defined in equation (12). However, this will not be the case during orbit night when there are no Sun sensor measurements or during orbit day if/when the Earth's magnetic field is aligned with the unit Sun vector. To handle these situations, inertial unit vectors $(\vec{U}_a, \vec{U}_b, \vec{U}_c)$ are established at the time of each update that are aligned with and in the direction of the vehicle axes (V_1, V_2, V_3), respectively. Hence, their components in vehicle axes are given by

$$\underline{U}_a = \begin{bmatrix} 1 \\ 0 \\ 0 \end{bmatrix} , \quad \underline{U}_b = \begin{bmatrix} 0 \\ 1 \\ 0 \end{bmatrix} , \quad \underline{U}_c = \begin{bmatrix} 0 \\ 0 \\ 1 \end{bmatrix} .$$

Their time derivatives, as seen by an observer rotating with the vehicle, will be approximated by

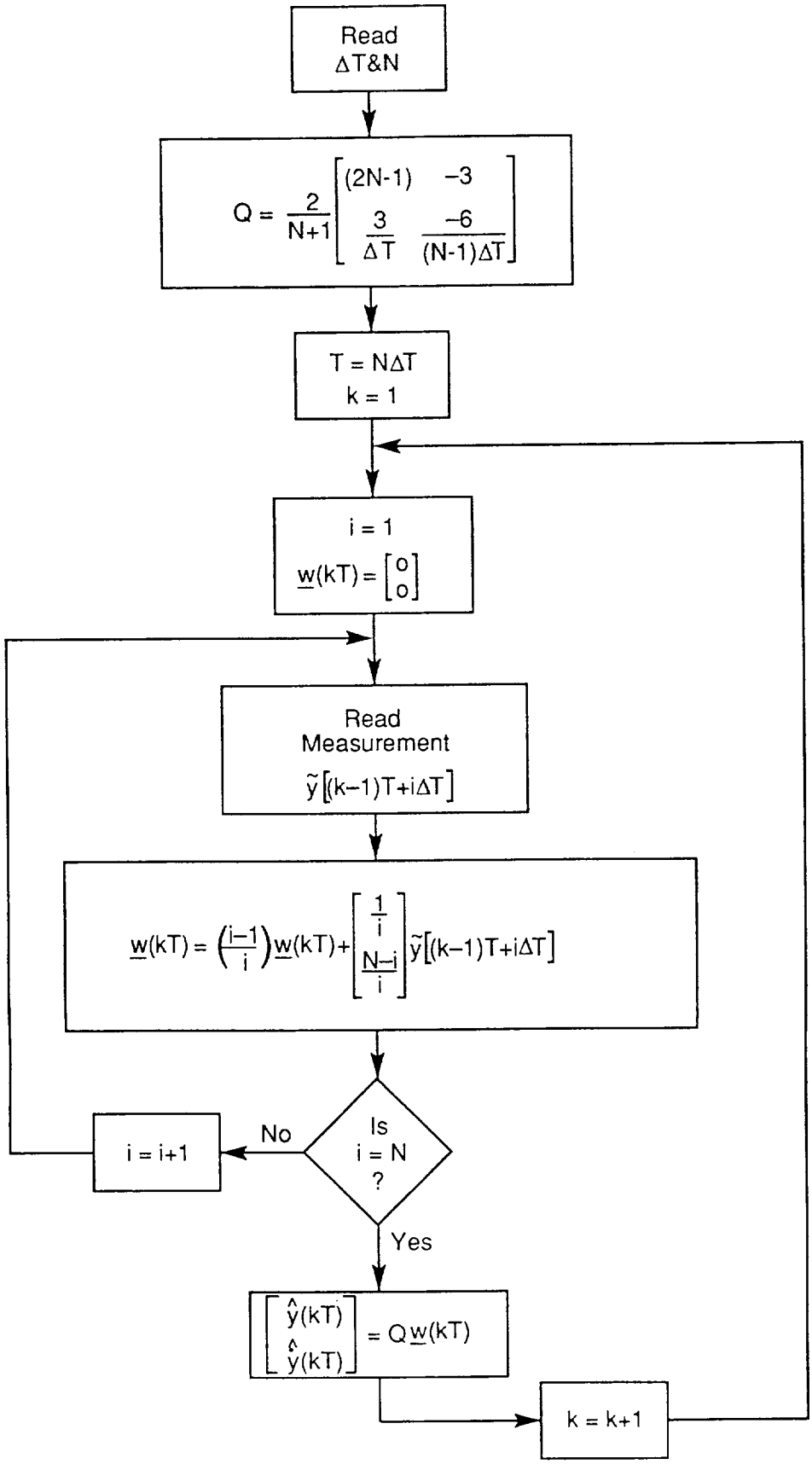

Figure 2. Logic flow chart for the scheme to estimate y and $\dot{y}$ every T seconds.

$$(\dot{\underline{U}}_a)_{\text{REL } V} = \tilde{\underline{U}}_a \hat{\underline{\omega}}_V(t_{n-}) = \begin{bmatrix} 0 \\ -\hat{\omega}_{V3}(t_{n-}) \\ \hat{\omega}_{V2}(t_{n-}) \end{bmatrix}$$

$$(\dot{\underline{U}}_b)_{\text{REL } V} = \tilde{\underline{U}}_b \hat{\underline{\omega}}_V(t_{n-}) = \begin{bmatrix} -\hat{\omega}_{V3}(t_{n-}) \\ 0 \\ \hat{\omega}_{V1}(t_{n-}) \end{bmatrix}$$

$$(\dot{\underline{U}}_c)_{\text{REL } V} = \tilde{\underline{U}}_c \hat{\underline{\omega}}_V(t_{n-}) = \begin{bmatrix} -\hat{\omega}_{V2}(t_{n-}) \\ \hat{\omega}_{V1}(t_{n-}) \\ 0 \end{bmatrix}$$

where $\hat{\underline{\omega}}_V(t_{n-1})$ denotes the estimated angular velocity based on the plant model, from equation (5) or (7), just prior to the update. $\underline{\delta}$ and τ are then augmented to include these, with their weighting factors set equal to 1 at all times. Hence, equations (11) and (12) become, respectively,

$$\underline{\delta} = \begin{bmatrix} \dfrac{k_B(\dot{\underline{B}})_{\text{REL } V}}{|\underline{B}|} \\ k_S(\dot{\underline{S}})_{\text{REL } V} \\ (\dot{\underline{U}}_a)_{\text{REL } V} \\ (\dot{\underline{U}}_b)_{\text{REL } V} \\ (\dot{\underline{U}}_c)_{\text{REL } V} \end{bmatrix},$$

and

$$\tau = \begin{bmatrix} \dfrac{k_B \tilde{\underline{B}}}{|\underline{B}|} \\ k_S \tilde{\underline{S}} \\ \tilde{\underline{U}}_a \\ \tilde{\underline{U}}_b \\ \tilde{\underline{U}}_c \end{bmatrix}.$$

This insures that, at all times, rank $[\tau] = 3$ and hence $\text{DET}[\tau^T \tau] \neq 0$, regardless of the number of inertial vectors measured or their relative orientation. Besides, it allows one measured inertial vector to partially update the estimated angular velocity and gives the latest estimate based on the plant model some weight in the update process, a la a Kalman filter. This helps to smooth the updated estimates with noisy sensor measurements.

To extend the update scheme to include star tracker measurements is straightforward; $\underline{\delta}$ and τ are augmented with terms similar to those for the Sun sensor measurements. Realize that reference star identification is not required; any star in the field-of-view can be tracked to get

useful measurement information, so long as it is tracked for the entire T-second interval between updates. When it leaves the field-of-view, another is found and tracked.

Other measurements such as look angles from tracking antennas or outputs from horizon sensors can also be used. They, too, are handled like Sun sensor measurements. Whether they are of benefit depends on how accurately angular velocity needs to be estimated and how good the measurements are.

C. Description of the Complete Estimation Scheme

A general logic flow chart for the complete estimation scheme is shown in figure 3. It assumes that momentum exchange devices are used for vehicle control; however, the changes to it when an RCS system is used are straightforward. It also shows a practical feature that has not been discussed until now. That is the capability of combining the estimated angular velocity with outputs from usable onboard rate gyros. This is applicable when one or two rate gyros still function and there is a desire to make maximum use of their precise measurements. This is handled by computing pseudo rate gyro outputs, $\hat{\omega}_G$, using the angular velocity estimates and the transformation matrix that defines the orientation of the onboard rate gyros relative to the vehicle axes. Then one or more pseudo rate gyros, specified by ground command, can be substituted for failed rate gyros in the normal rate gyro computations. The pseudo rate gyros may also be useful in detecting failures in the usable rate gyros.

III. APPLICATION TO THE HUBBLE SPACE TELESCOPE

The HST has six single-axis rate gyros, mounted so that any three of the six allow reconstruction of the vehicle angular velocity in all three axes.[11] As of August 1991, two had already failed and a third exhibited intermittent abnormal behavior.[3] Should four or more fail, vehicle control would be in jeopardy. To prepare for the worst, a study was performed to see if vehicle control could be maintained with four or more failed. The approach was to use the HST Sun point mode with a minimum of modification and the scheme described in section II for estimating angular velocity. The HST Sun point mode autonomously slews and points the vehicle at the Sun to maintain a power positive condition when onboard failures are detected.[12] If this could be done with fewer than three rate gyros, eventually new ones could be delivered on a space shuttle refurbishment mission and normal operation restored. The results of that study are described below. To make them meaningful, some description of the HST and its normal Sun point mode are needed first.

Figure 4 shows a drawing of the HST and its vehicle axes (V_1,V_2,V_3).[11] It has coarse Sun sensors (CSS's) looking out the $+V_1$, $-V_1$, and $+V_3$ axes. It has another with its line-of-sight at a 45° angle to the $-V_1$ and the $-V_3$ axes. The linear range of each sensor has a half-cone angle of approximately 38°. The total field-of-view of each is about 2π steradians. Their outputs are sampled once-per-second by the onboard control computer and used for acquiring and pointing the $+V_3$ axis or the $-V_1$ axis at the Sun, in the normal Sun point mode. Quantization due to the A/D conversion is 0.36° in each axis of each sensor.

The HST also has three fixed head star trackers (FHST's) that are used for coarse attitude determination during normal operation. One looks out the $-V_3$ axis. The other two are

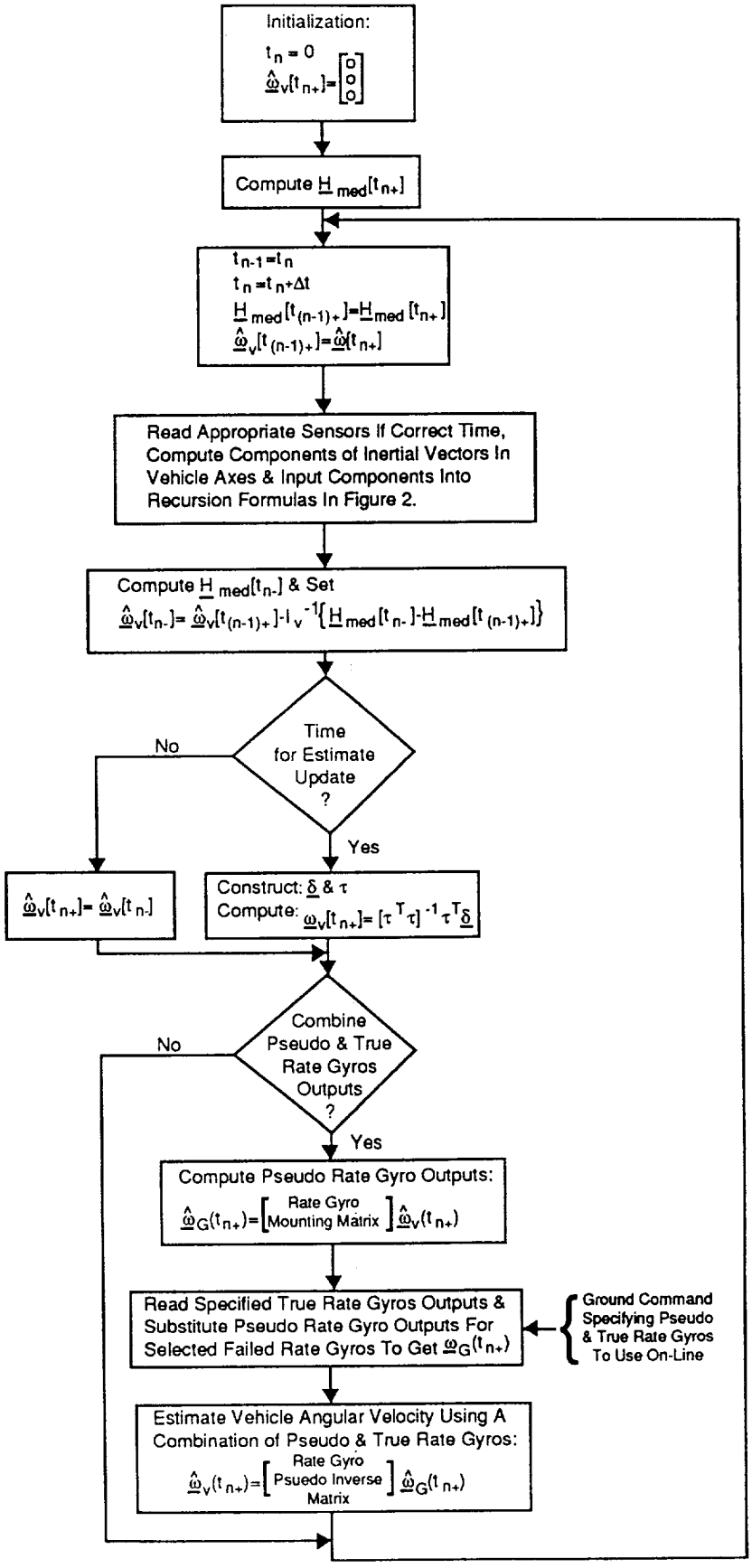

Figure 3. Logic flow chart for the complete estimation scheme with momentum exchange devices for control

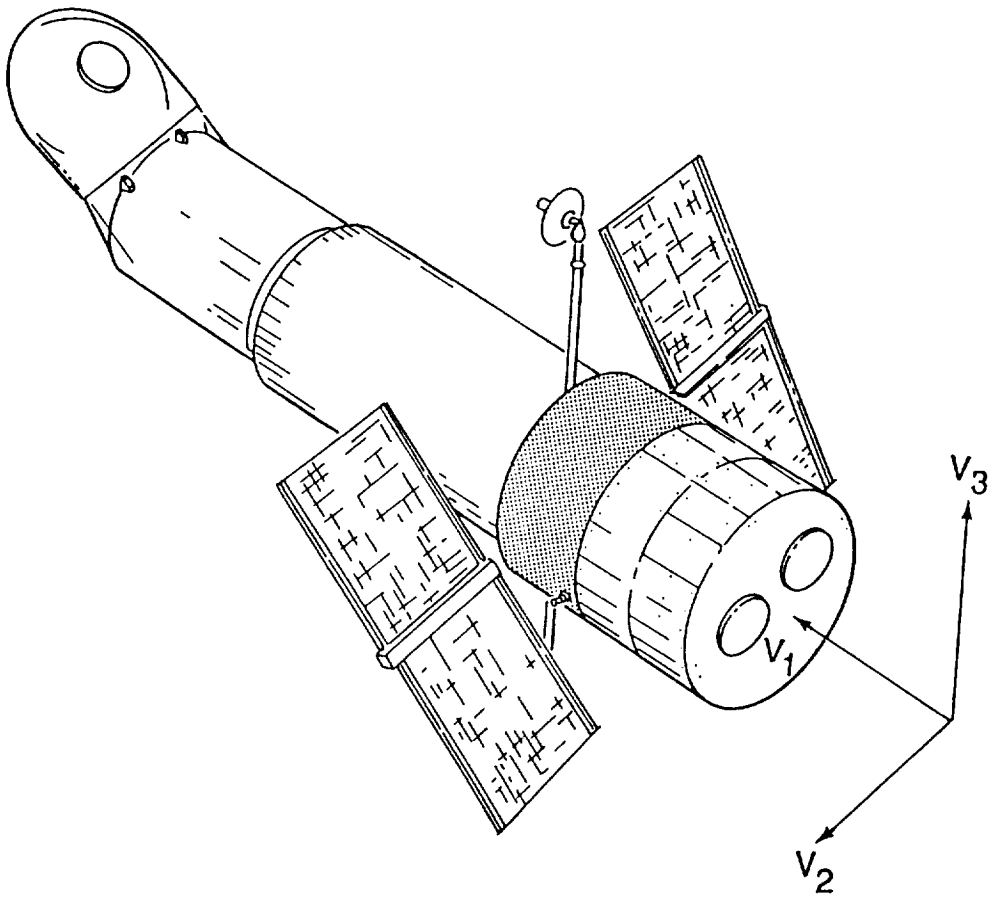

Figure 4. Hubble space telescope and its vehicle axes.

skewed 49° from the $-V_3$ axis toward the $-V_1$ axis and make an angle of 44° with respect to each other. The field-of-view of each is 8.5°×8.5°. Their outputs are sampled by the control computer every 0.1 s and quantized to 7.5 arcsec in each axis. If an FHST looks within about 15° of the Sun or the bright Earth's limb, its shutter automatically closes. There is a redundant pair of magnetometers onboard for measuring the Earth's magnetic field in vehicle axes. These are used in a magnetic torquing system that generates low-amplitude low-frequency torques on the vehicle for desaturating a set of four reaction wheels. The magnetometer outputs are sampled every 1 s by the control computer and quantized to 4.7 milli-gauss.

The reaction wheels generate control torques for vehicle attitude control during normal operation, as well as in the Sun point mode. Wheel speeds are measured with tachometers that are sampled by the control computer every 0.025 s and quantized to 3.75 revolutions per minute (r/m), effectively. The maximum wheel speed of each is 3,000 r/m.

In the normal Sun point mode, the control computer software logic slews the vehicle to get the sunline in the V_1–V_3 plane. Concurrently, it slews the vehicle about the V_2 axis at 0.25°/s until the sunline is in the field-of-view of the CSS designated for Sun pointing. This can be either the one looking out the $+V_3$ axis or the $-V_1$ axis. At this point, the control system in two axes uses outputs from this CSS for position feedback and angular velocity from the rate gyros for rate feedback. The third axis is similar except that integrated velocity is used for position. When the vehicle enters orbit night, integrated velocity is used for position feedback in all three axes. In each axis, the linearized closed-loop system looks like a second-order system with the position and rate control law gains chosen so $\omega_n \doteq 0.004$ Hz and $\zeta \doteq 0.707$.

With this as the normal Sun point mode, a modified version of it was defined that would work with four or more of the rate gyros failed. In this modified version, the normal Sun point logic and software are left intact, with the following exceptions. First, only $+V_3$ Sun point is used. With the $+V_3$ axis pointed at the Sun during orbit day, the FHST looking out the $-V_1$ axis is unobstructed by the Earth during orbit night. Then, it is almost always assured of finding a suitable reference star in its field-of-view. Measurements from it are used in place of CSS outputs in the control laws for the V_1 and V_2 axes, in order to hold the $+V_3$ axis close to the sunline during orbit night. Also, this practically insures good estimates for angular velocity in the critical axes for Sun pointing, V_1 and V_2, over the entire course of each orbit. Besides, this has little impact on the existing software, but significantly enhances the robustness of the scheme. The only other change to the software is that angular velocity is estimated using the scheme presented in section II and, specifically, the logic flow chart shown in figure 3. Measurements from the CSS's, the FHST's, and the magnetometers are used in the estimate updates which occur every 10 seconds. CSS and magnetometer measurements are input into the recursion formulas in figure 2 every 1 s. FHST measurements are input every 0.1 s.

A computer simulation of this modified Sun point scheme was developed to test its performance. The simulation has vehicle rigid body dynamics, aerodynamic and gravity gradient torques, a six displaced-dipole model for the Earth's magnetic field, and sensor quantization as described previously. It simulates vehicle orbit day and night relative to the CSS's and FHST's. If the HST is in orbit day and the Sun is in the linear range of a CSS, the weighting factor k_S is set equal to 1; otherwise, k_S is 0. If an FHST is within 15° of the Sun or the Earth's limb, its shutter closes momentarily and its weighting factor is set equal to 0. If an FHST is tracking a reference star and the star leaves the field-of-view sometime during a 10-s interval, that FHST's weighting factor is set to 0 for the subsequent update. Otherwise, its weighting factor is set equal to 20. A large value is chosen because the FHST's are much more accurate than the other sensors. When an FHST is tracking a star that leaves its field-of-view, a new one is assumed to be found in the center. The magnetometer is only used in estimating angular velocity until the Sun is in the linear range of the CSS looking out the $+V_3$ axis. After that, it is no longer used. Hence, k_B equals 1 before Sun acquisition and 0 afterwards. This is done because angular velocity estimated with the magnetometer is less accurate than that estimated with the CSS's or FHST's, since the direction of the Earth's field varies with the position of the vehicle in orbit. The error in estimated velocity using the magnetometer can be as much as 0.1°/s, but this is still accurate enough for Sun acquisition. Besides, after Sun acquisition, the magnetometer measurements are no longer needed.

In the simulation, a difficult set of initial conditions was defined to test the modified Sun point scheme with all rate gyros failed. The day of year was set equal to 80 (vernal equinox), the longitude of the ascending node for the orbit was 90°; the vehicle had about 450 s to go before entering orbit night; the initial vehicle angular velocity was 0.3°/s in each axis; the $+V_3$ axis was about 170° from the Sun line. For these initial conditions, simulation results are shown in figures 5 to 10. Figure 5 shows the angle between the $+V_3$ axis and the sunline. Figures 6 to 8 show the estimated and true angular velocities in each axis. Figure 9 shows the weighting factors k_B for the magnetometer and k_S for the CSS's. It also indicates the periods of orbit day, by a 1, and periods of orbit night, by a 0. Figure 10 shows the weighting factors for the FHST's, where k_{SA} corresponds to the FHST looking out the $-V_3$ axis.

The results show that the modified Sun point scheme with the new rate estimator performs quite well, in spite of the difficult initial conditions. The time it takes for the $+V_3$ axis to reach and stay within 10° of the sunline is about 800 s after reentering orbit day. The angular

velocity in each axis is estimated to within about 0.01°/s, once $k_B = 0$. Before that, it is estimated to within about 0.05°/s, which is adequate for Sun acquisition.

For comparison, simulation results were obtained with the true angular velocity used for control in place of the estimated, and with everything else the same. These results are presented in figures 11 to 14, and show just how well the modified Sun point scheme works with the new estimator.

Finally, two additional cases were run with these same initial conditions except: in the first, the angular velocity used for control was estimated based on two pseudo and one true rate gyros; in the second, it was based on one pseudo and two true rate gyros. These tested the option of combining psuedo and true rate gyro measurements to get estimated angular velocity by the procedure shown in figure 3. This is useful with one or two true rate gyros still operating. The simulation results for these cases were similar to the previous ones, lying somewhere in between the two, as one might expect.

IV. FINAL COMMENTS

This paper has presented a new scheme for estimating the angular velocity of a spacecraft without using rate gyros. It is shown to be useful for maintaining spacecraft attitude control in an emergency, when all or most of the onboard rate gyros have failed. However, it may also have application in spacecraft that wish to avoid the spinning rotors which are an integrable part of most rate gyros. For example, take the Gravity Probe-B spacecraft.[13] It requires an extremely low-g environment onboard, for scientific reasons, and residual mass unbalance in the spinning rotors could possibly produce accelerations that are unacceptable.

Another potential use for the new estimator is in online failure detection of onboard rate gyros. The pseudo rate gyro outputs derived from estimated angular velocity could be compared with true rate gyro outputs as a means of detecting rate gyro failures. This is an area for further study.

Another area for further study is to investigate techniques for optimizing the weighting factors in the estimate update scheme. It should be possible to choose them to minimize the variance of the estimation errors, a la a Kalman filter. If this cannot be done analytically, then surely it is possible by means of simulation.

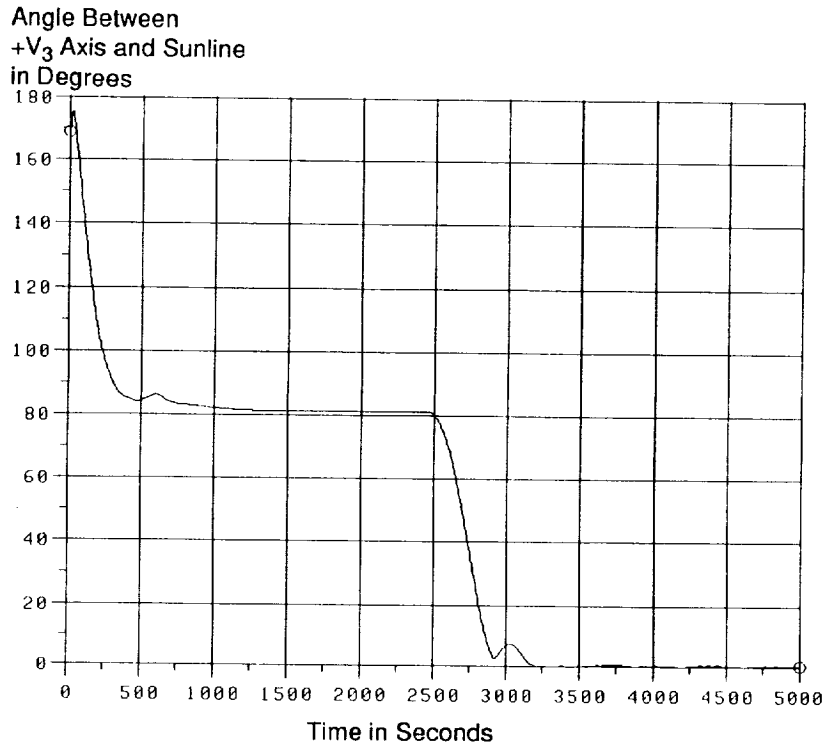

Figure 5. Angle between $+V_3$ axis and Sun line, using estimated angular velocity for control.

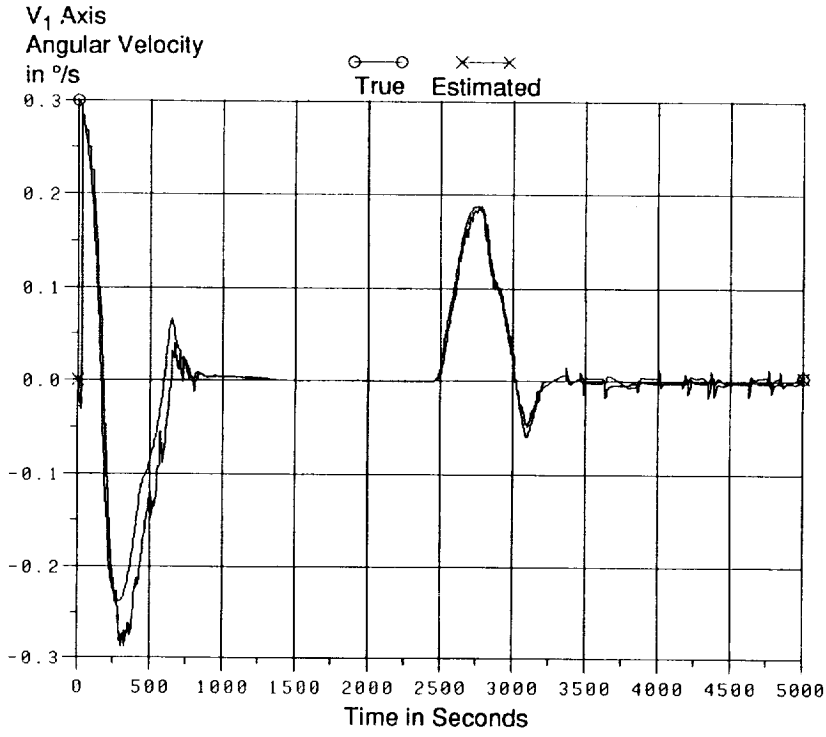

Figure 6. Estimated versus true angular velocity in V_1 axis, using estimated angular velocity for control.

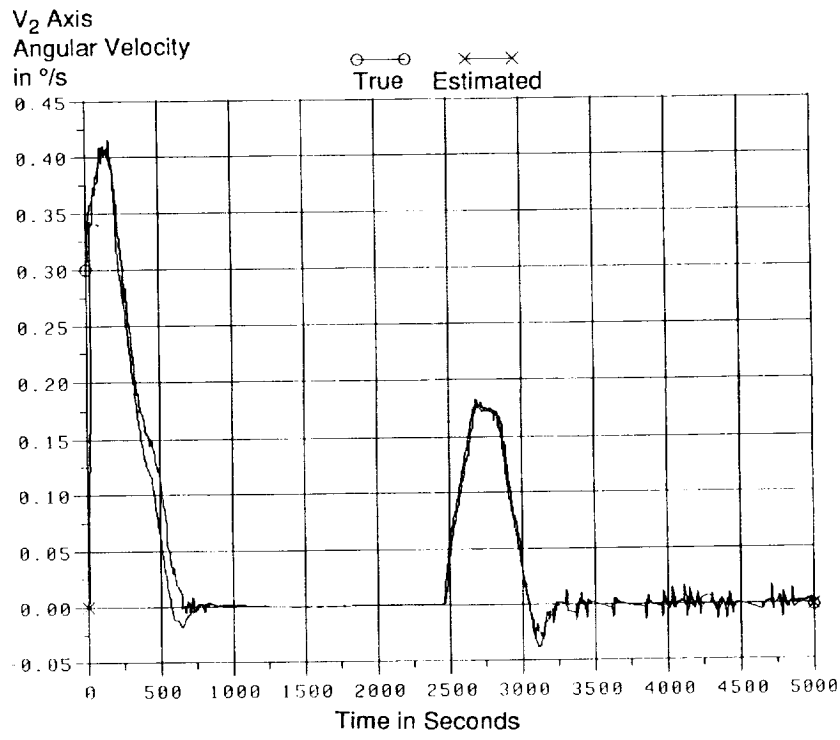

Figure 7. Estimated versus true angular velocity in V_2 axis, using estimated angular velocity for control.

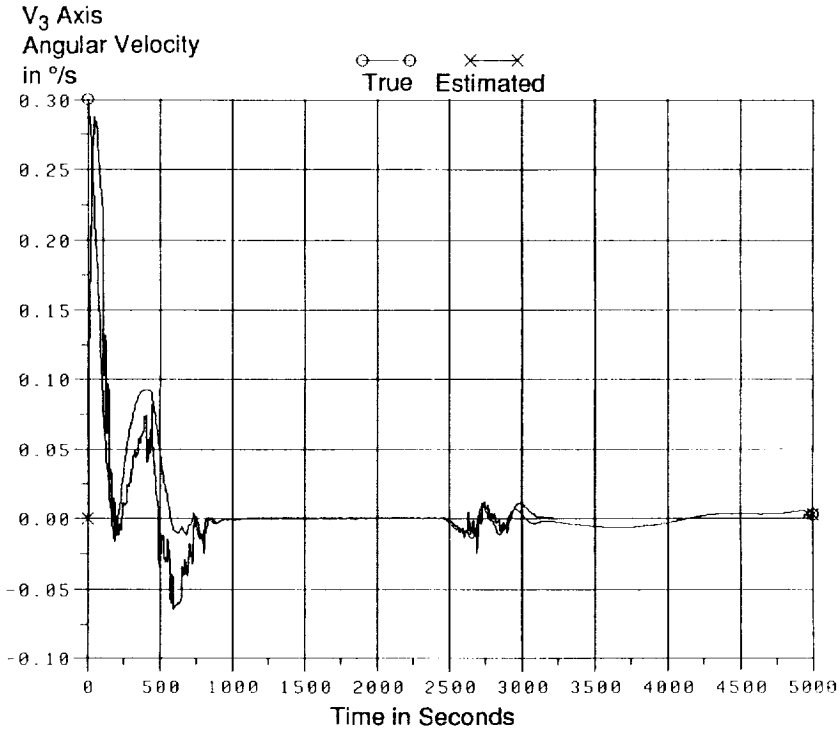

Figure 8. Estimated versus true angular velocity in V_3 axis, using estimated angular velocity for control.

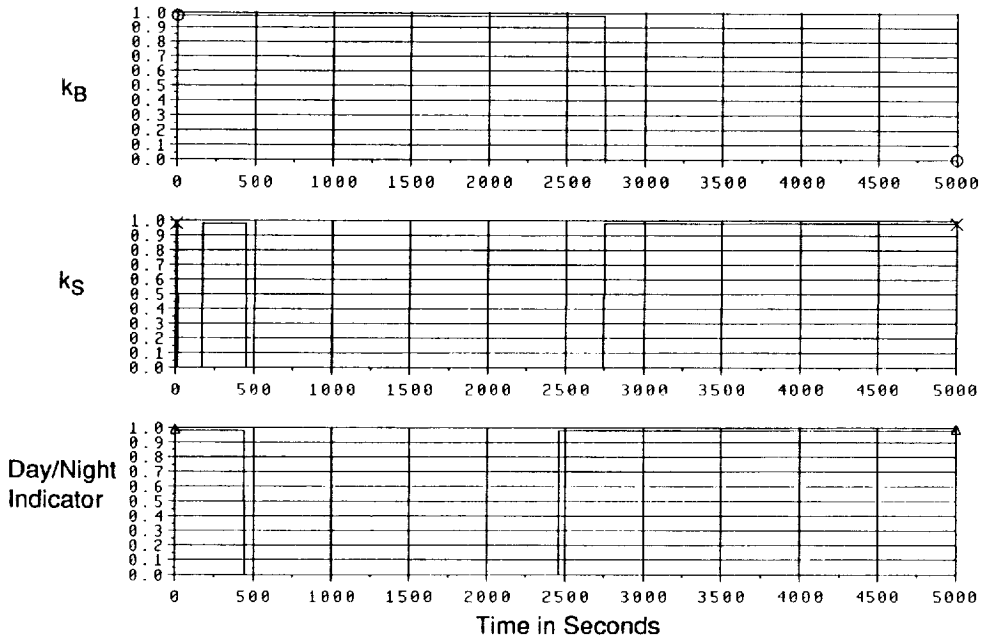

Figure 9. Weighting factors for the magnetometers and Sun sensors and orbit day/night indicator, using estimated angular velocity for control.

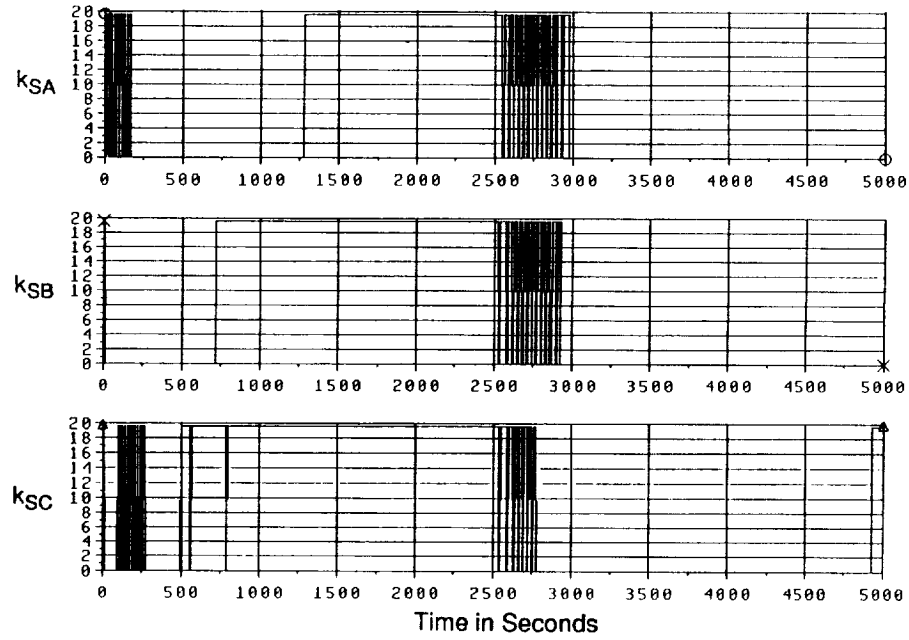

Figure 10. Weighting factors for the fixed head star trackers, using estimated angular velocity for control.

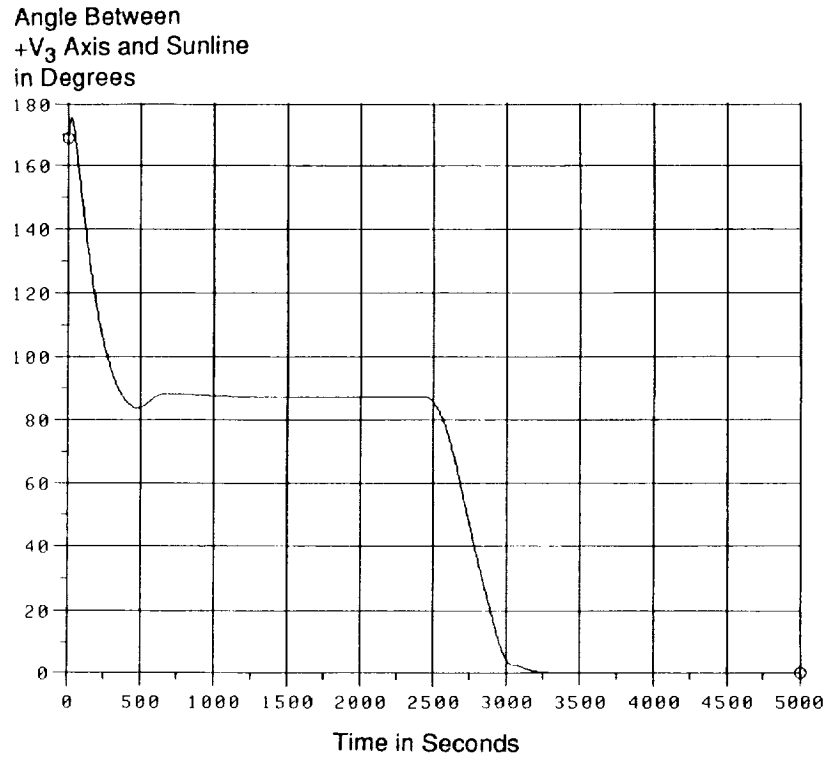

Figure 11. Angle between $+V_3$ axis and Sun line, using true angular velocity for control.

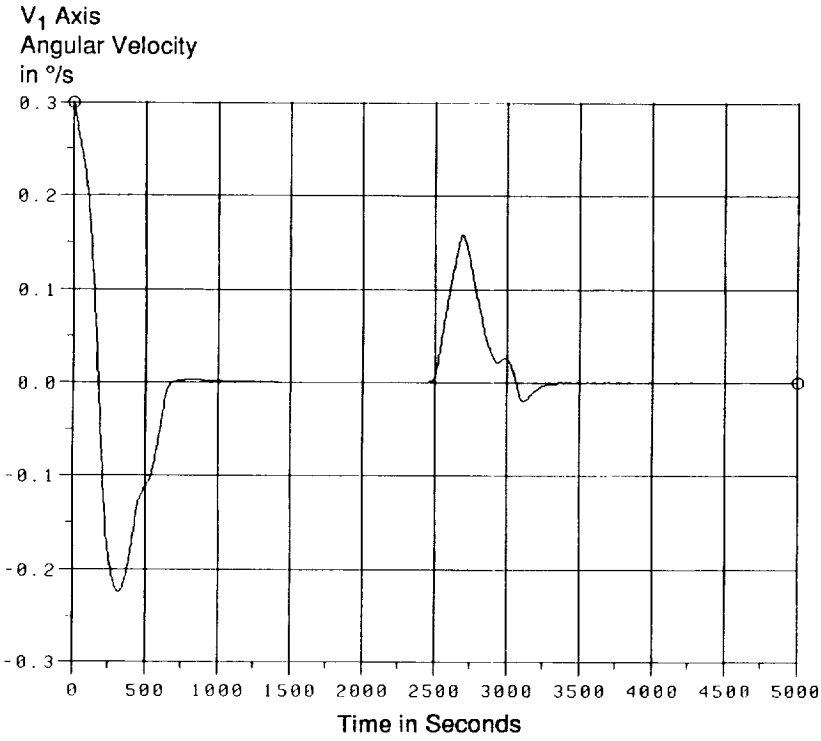

Figure 12. True angular velocity in V_1 axis, using true angular velocity for control.

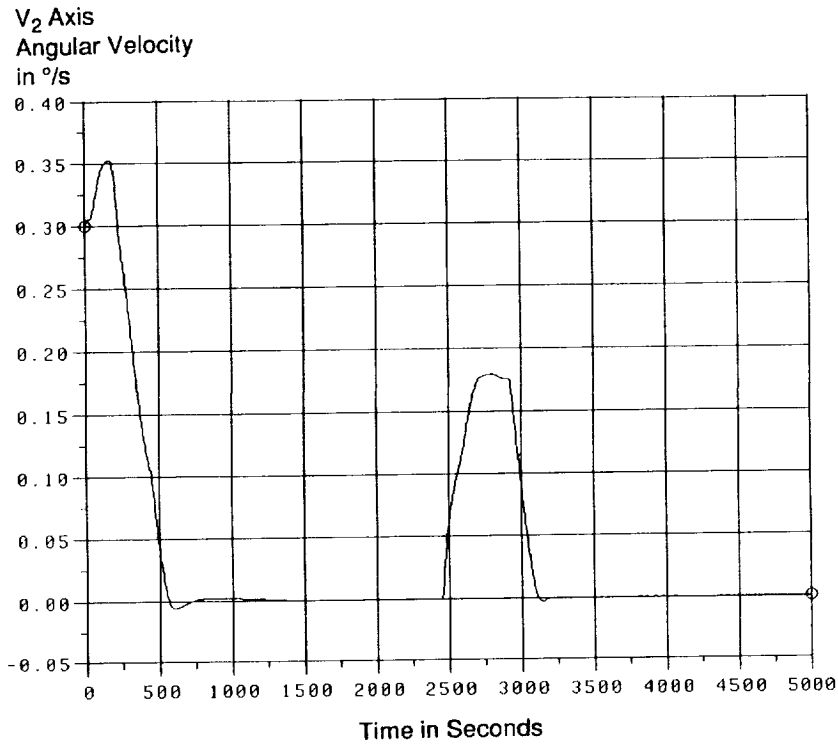

Figure 13. True angular velocity in V_2 axis, using true angular velocity for control.

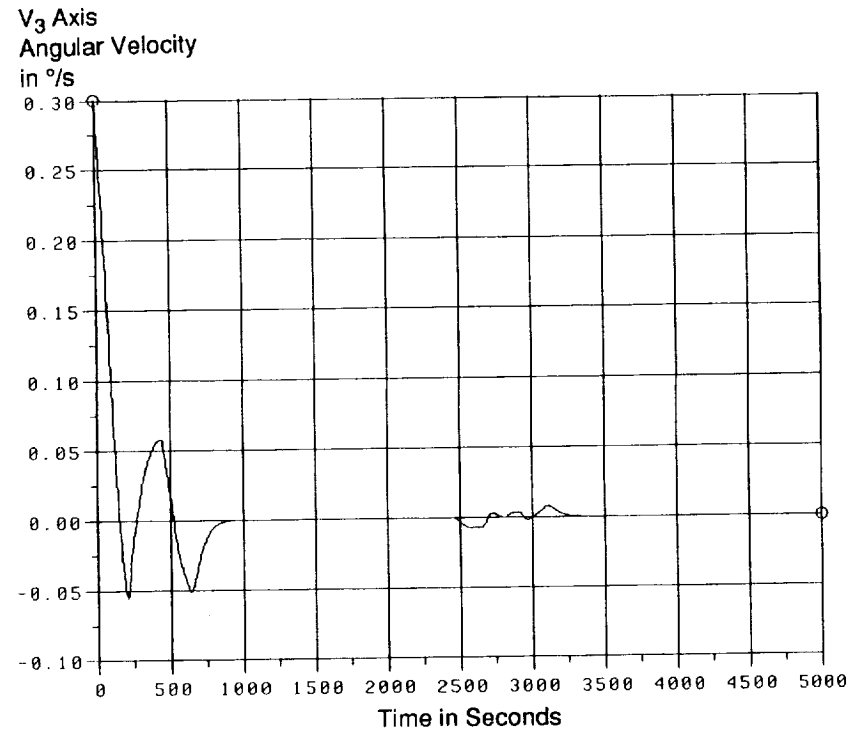

Figure 14. True angular velocity in V_3 axis, using true angular velocity for control.

REFERENCES

1. Chubb, W.B., Kennel, H.F., Rupp, C.C., and Seltzer, S.M.: "Flight Performance of Skylab Attitude and Pointing Control System." NASA TN D-8003, Marshall Space Flight Center, AL, June 1975.

2. Femiano, M.D.: "Inflight Redesign of the IUE Attitude Control System." Proceedings of the AIAA Space Systems Technology Conference, San Diego, CA, June 9–12, 1986, pp. 164–170.

3. "Science News," vol. 140, No. 6, August 10, 1991, p. 86.

4. Farrell, J.L.: "Attitude Determination by Kalman Filtering." Automatica, vol. 6, No. 3, 1970, pp. 419–430.

5. Chang, Chaw-Bing, and Tabaczynski, J.A.: "Application of State Estimation to Target Tracking." IEEE Transactions on Automatic Control, vol. AC-29, No. 2, February 1984, pp. 98–109.

6. Gelb, A.: "Applied Optimal Estimation." The M.I.T. Press, Cambridge, MA, 1984, pp. 151–152.

7. Zwartbol, T., Van Den Dam, R.F., Terpstra, A.P., and Van Woerkom, P.T.: "Attitude Estimation and Control of Maneuvering Spacecraft." Automatica, vol. 21, No. 5, 1985, pp. 513–526.

8. Wertz, J.R.: "Spacecraft Attitude Determination and Control." Reidel, Boston, MA, 1986, pp. 437–469.

9. Greenwood, D.T.: "Principles of Dynamics." Prentice-Hall, Englewood Cliffs, NY, 1988.

10. Polites, M.E.: "A New Scheme for Processing Noisy Star Tracker Measurements in Spacecraft Attitude Determination Systems." Proceedings of the AIAA Guidance, Navigation, and Control Conference, New Orleans, LA, August 12–14, 1991, pp. 917–924.

11. Beals, G.A., Crum, R.C., Dougherty, H.I., Hegel, D.K., Kelley, J.L., and Rodden, J.J.: "Hubble Space Telescope Precision Pointing Control Systems." Journal of Guidance, Control, and Dynamics, vol. 11, No. 2, March–April 1988, pp. 119–123.

12. Dougherty, H., Machnick, J., Nakashima, A., Henry, J., and Tompetrini, K.: "Magnetic Control Systems for Large Spacecraft With Application to Space Telescope." Proceedings of the Annual Rocky Mountain Guidance and Control Conference, Keystone, CO, January 31–February 4, 1981, pp. 95–116.

13. Parkinson, B.W., and Kasdin, N.J.: "Twenty Milliarcsec Pointing System for the Rolling GP-B Spacecraft." Proceedings of the Annual Rocky Mountain Guidance and Control Conference, Keystone, CO, January 30–February 3, 1988, pp. 65–89.

REPORT DOCUMENTATION PAGE

Form Approved
OMB No. 0704-0188

1. AGENCY USE ONLY (Leave blank)	2. REPORT DATE	3. REPORT TYPE AND DATES COVERED
	December 1991	Technical Paper

4. TITLE AND SUBTITLE
A Nonlinear Estimator for Reconstructing the Angular Velocity of a Spacecraft Without Rate Gyros

5. FUNDING NUMBERS

6. AUTHOR(S)
M.E. Polites and W.D. Lightsey

7. PERFORMING ORGANIZATION NAME(S) AND ADDRESS(ES)
George C. Marshall Space Flight Center
Marshall Space Flight Center, Alabama 35812

8. PERFORMING ORGANIZATION REPORT NUMBER
M-675

9. SPONSORING / MONITORING AGENCY NAME(S) AND ADDRESS(ES)
National Aeronautics and Space Administration
Washington, DC 20546

10. SPONSORING / MONITORING AGENCY REPORT NUMBER
NASA TP-3178

11. SUPPLEMENTARY NOTES
Prepared by Structures and Dynamics Laboratory, Science and Engineering Directorate.

12a. DISTRIBUTION / AVAILABILITY STATEMENT
Unclassified – Unlimited
Subject Category 31

12b. DISTRIBUTION CODE

13. ABSTRACT *(Maximum 200 words)*

This paper presents a new scheme for estimating the angular velocity of a spacecraft without rate gyros. It is based upon a nonlinear estimator whose inputs are measured inertial vectors and their calculated time-derivatives relative to vehicle axes. It works for all spacecraft attitudes and requires no knowledge of attitude. It can use measurements from a variety of onboard sensors like Sun sensors, star trackers, or magnetometers, and in concert. It can also use look angle measurements from onboard tracking antennas for tracking and data relay satellites or global positioning system satellites. In this paper, it is applied to a Sun point scheme on the Hubble space telescope assuming all or most of its onboard rate gyros have failed. Simulation results are presented which verify it.

14. SUBJECT TERMS	15. NUMBER OF PAGES
Angular Velocity, Hubble Space Telescope, Nonlinear Estimation, Rate Gyro Failures, Spacecraft	24
	16. PRICE CODE A03

17. SECURITY CLASSIFICATION OF REPORT	18. SECURITY CLASSIFICATION OF THIS PAGE	19. SECURITY CLASSIFICATION OF ABSTRACT	20. LIMITATION OF ABSTRACT
Unclassified	Unclassified	Unclassified	Unlimited

NSN 7540-01-280-5500

Standard Form 298 (Rev. 2-89)
Prescribed by ANSI Std. Z39-18
298-102

NASA-Langley, 1991